Quantum computing with spin qubits interacting through delocalized excitons: Overcoming hole mixing

Brendon W. Lovett,[1,*] Ahsan Nazir,[1] Ehoud Pazy,[2] Sean D. Barrett,[3] Timothy P. Spiller,[3] and G. Andrew D. Briggs[1]
[1]*Department of Materials, Oxford University, Oxford OX1 3PH, United Kingdom*
[2]*Chemistry Department, Ben-Gurion University of the Negev, P.O. Box 653, Beer-Sheva 84105, Israel*
[3]*Hewlett-Packard Laboratories, Filton Road, Stoke Gifford, Bristol BS34 8QZ, United Kingdom*
(Received 6 May 2005; revised manuscript received 22 July 2005; published 20 September 2005)

As a candidate scheme for controllably coupled qubits, we consider two quantum dots, each doped with a single electron. The spin of the electron defines our qubit basis and trion states can be created by using polarized light; we show that the form of the excited trion depends on the state of the qubit. By using the Luttinger-Kohn Hamiltonian we calculate the form of these trion states in the presence of light-heavy hole mixing, and show that they can interact through both the Förster transfer and static dipole-dipole interactions. Finally, we demonstrate that by using chirped laser pulses, it is possible to perform a two-qubit gate in this system by adiabatically following the eigenstates as a function of laser detuning. These gates are robust in that they operate with any realistic degree of hole mixing, and for either type of trion-trion coupling.

DOI: 10.1103/PhysRevB.72.115324 PACS number(s): 78.67.Hc, 73.20.Mf, 03.67.Lx

I. INTRODUCTION

In the quest for a solid state quantum information processor, there is great attraction in combining the relatively long coherence times of spins with the speed and versatility of optical manipulation. There have been many papers describing different ways to embody a qubit by using the two levels of a confined spin-1/2 electron.[1–6] The direct interaction between two such spin qubits is often quite weak, but they can be enhanced by exploiting degrees of freedom which lie outside the computation Hilbert space. For example, spin information can be transferred to spatial degrees of freedom in a double quantum dot structure,[6] or to photons in an electromagnetic cavity.[7] Recent proposals[8–10] have described ways in which spins might be coupled by using polarized light to selectively create trion states. Such spin selective charge excitations benefit directly from the recent progress in ultrafast optoelectronics: both the coherent manipulation of excitons in quantum dots (QDs) (Refs. 11–13) and spin selective optical transitions[14] have been demonstrated. Moreover, once a gate operation is complete, it is possible to arrange that all population returns to the qubit subspace, and the quantum device therefore benefits from the robust coherence properties[15–17] of the electron spin.

In Ref. 10, we demonstrated that an entangling CPHASE gate can be performed between single spins on each of two adjacent QDs by the spin selective excitation of a single, delocalized, exciton. The required delocalization occurs when the dots are (near) resonant, and if they interact through the Förster energy transfer mechanism.[18,19] The proposal is based on the Pauli blocking mechanism[20] and is valid only in the special case of *no light-heavy hole mixing*, which, though sometimes applicable,[21] is not generally true for most QD systems.[22] We shall here demonstrate an alternative method of performing a two-qubit gate, which solves this problem. Following Ref. 9, it is based on using chirped laser pulses to perform adiabatic quantum gate operations.

To develop this model, the following steps are necessary. We shall first describe how the QDs employed in our quantum information implementation scheme are modeled. We describe the hole sub-band mixing in terms of a four band Luttinger-Kohn model,[23] and show how this affects the coupling of confined charge carriers to a laser field (Sec. II). We then consider a coupled QD system and present the dependence of the Förster transfer operator on the angular momenta of the excitonic states which it connects. We shall derive the form of the Förster transfer interaction for two coupled trions and hence write down an effective Hamiltonian for two interacting QDs coupled to a laser field, in the presence of hole mixing (Sec. III). The proposal for performing quantum gates by creating trions adiabatically is then discussed (Sec. IV), and we describe two different modes in which the two qubit gate can be operated. We shall demonstrate that the adiabatic scheme circumvents the hole mixing problem and briefly discuss why it should also reduce phonon decoherence. State measurement, preparation and scalability will be discussed next (Sec. V) and then we summarize (Sec. VI).

II. SINGLE QUANTUM DOT MODEL

Let us consider self-assembled QDs with strong confinement along the growth direction z, which is also the QD symmetry axis. This type of QD can be produced in materials such as InGaAs by using the Stranski-Krastanow method,[24] which may allow the realization of a controllably coupled many dot system. Such QDs exist in the strong confinement regime, in which the typical size, L, of the QD in the growth direction is of the order of 10–20 nm. In this regime, the Coulomb interaction between charge carriers scales as $1/L$, but the single-particle excitation energy has a $1/L^2$ dependence. Excitonic wave functions can therefore be modelled by products of single particle electron and hole states, with Coulomb effects being introduced by using first order perturbation theory. This approximation results in a shift to the excitonic energy but does not lead to the entanglement of electron and hole. The effective mass and en-

velope function approximations reveal that the electronic states inside the QD exhibit atomiclike symmetries, which have been identified experimentally.[25]

The wave function for a single particle in a QD can be described by a product of a *Bloch function U*, which has the periodicity of the atomic lattice, and an *envelope function* ϕ, which describes the amplitude modulation of the wave function that is imposed by the confinement potential. Henceforth we shall only consider the lowest energy envelope function for both the conduction and valence bands (which has no nodes in both cases), and neglect any mixing with higher envelopes. This approximation is discussed in Ref. 26: we use it for clarity and our scheme does not depend on it; a more thorough desciption of the electronic structure of self-assembled QDs is presented in Ref. 27.

The eigenstates of the angular momentum operators, $\hat{J}$ and $\hat{J}_z$ for the six hole states closest to the top of the valence band can be represented by[28]

$$|3/2_h,3/2\rangle = \frac{f_{hh}(r)}{\sqrt{2}}|(X+iY)\alpha\rangle, \tag{1}$$

$$|3/2_h,-3/2\rangle = \frac{f_{hh}(r)}{\sqrt{2}}|(X-iY)\beta\rangle, \tag{2}$$

$$|3/2_h,1/2\rangle = \frac{f_{lh}(r)}{\sqrt{6}}[|(X+iY)\beta\rangle - |2Z\alpha\rangle], \tag{3}$$

$$|3/2_h,-1/2\rangle = \frac{f_{lh}(r)}{\sqrt{6}}[|(X-iY)\alpha\rangle + |2Z\beta\rangle], \tag{4}$$

$$|1/2_h,1/2\rangle = -\frac{f_{\mathrm{so}}(r)}{\sqrt{3}}[|(X+iY)\beta\rangle + |Z\alpha\rangle], \tag{5}$$

$$|1/2_h,-1/2\rangle = -\frac{f_{\mathrm{so}}(r)}{\sqrt{3}}[|(X-iY)\alpha\rangle - |Z\beta\rangle]. \tag{6}$$

We have labeled the Bloch functions U by using the notation $|J_h,J_z\rangle$. The first two states correspond to heavy holes (hh), the next two are light holes (lh), and the last two are split-off holes (so). The functions f_i describe the radial dependence of each Bloch function type $i \in \{hh,lh,\mathrm{so}\}$; α and β are the up and down spin states respectively. The X, Y, and Z represent orbital wave functions as follows:

$$\langle \mathbf{r}|X\rangle = \sqrt{\frac{3}{4\pi}}\sin\theta\cos\phi, \tag{7}$$

$$\langle \mathbf{r}|Y\rangle = \sqrt{\frac{3}{4\pi}}\sin\theta\sin\phi, \tag{8}$$

$$\langle \mathbf{r}|Z\rangle = \sqrt{\frac{3}{4\pi}}\cos\theta. \tag{9}$$

The electron states are simply

$$|1/2_e,1/2\rangle = g(r)|S\alpha\rangle, \tag{10}$$

$$|1/2_e,-1/2\rangle = g(r)|S\beta\rangle. \tag{11}$$

$\langle \mathbf{r}|S\rangle = 1/\sqrt{4\pi}$ is the isotropic orbital function and $g(r)$ is the radial dependence of the electron's wave function.

We now note that

$$\int \langle \mathbf{r}|X\rangle x\langle \mathbf{r}|S\rangle d\Omega = \int \langle \mathbf{r}|Y\rangle y\langle \mathbf{r}|S\rangle d\Omega = \int \langle \mathbf{r}|Z\rangle z\langle \mathbf{r}|S\rangle d\Omega = \frac{r}{\sqrt{3}}, \tag{12}$$

where $d\Omega$ is the infinitesimal solid angle. We also see that

$$\int \langle \mathbf{r}|X\rangle y\langle \mathbf{r}|S\rangle d\Omega = \int \langle \mathbf{r}|X\rangle z\langle \mathbf{r}|S\rangle d\Omega = 0, \tag{13}$$

$$\int \langle \mathbf{r}|Y\rangle x\langle \mathbf{r}|S\rangle d\Omega = \int \langle \mathbf{r}|Y\rangle z\langle \mathbf{r}|S\rangle d\Omega = 0, \tag{14}$$

$$\int \langle \mathbf{r}|Z\rangle x\langle \mathbf{r}|S\rangle d\Omega = \int \langle \mathbf{r}|Z\rangle y\langle \mathbf{r}|S\rangle d\Omega = 0. \tag{15}$$

These relations will be important in the following discussion.

A. Hole mixing

Most semiconductors exhibit mixing of the heavy and light hole sub-bands, which we shall now describe by using the Luttinger-Kohn model.[23] The electron eigenstates of bulk semiconductors may be characterized by the crystal momentum wave vector, $\mathbf{k}=\{k_x,k_y,k_z\}$. The coupling between light and heavy holes is described by a four band Luttinger-Kohn Hamiltonian,[23] so long as the split off holes are energetically distant enough that coupling to this band can be neglected.[28] In the basis $\{|J_z=+3/2\rangle,|J_z=+1/2\rangle,|J_z=-1/2\rangle,|J_z=-3/2\rangle\}$, the Hamiltonian is written

$$\mathcal{H} = \begin{pmatrix} H_{hh} & -b & -c & 0 \\ -b^* & H_{lh} & 0 & -c \\ -c^* & 0 & H_{lh} & b \\ 0 & -c^* & b^* & H_{hh} \end{pmatrix}. \tag{16}$$

The uncoupled heavy hole Hamiltonian, H_{hh} is

$$H_{hh} = \frac{\hbar^2 k_z^2}{2m_0}(\gamma_1 - 2\gamma_2) + \frac{\hbar^2(k_x^2+k_y^2)}{2m_0}(\gamma_1+\gamma_2). \tag{17}$$

The uncoupled light hole Hamiltonian, H_{lh} is

$$H_{ll} = \frac{\hbar^2 k_z^2}{2m_0}(\gamma_1 + 2\gamma_2) + \frac{\hbar^2(k_x^2+k_y^2)}{2m_0}(\gamma_1-\gamma_2). \tag{18}$$

The mixing parameters are

$$c = \frac{\sqrt{3}\hbar^2}{2m_0}[\gamma_2(k_x^2-k_y^2) - 2i\gamma_3 k_x k_y] \tag{19}$$

and

$$b = \frac{\sqrt{3}\hbar^2}{m_0}\gamma_3 k_z(k_x - ik_y). \tag{20}$$

γ_1, γ_2, and γ_3 are the Luttinger parameters[28,29] and m_0 is the free electron mass.

For the quantum confined states that are found in semiconductor nanostructures, the crystal momentum is no longer a good quantum number. It is therefore necessary to replace each component of $\mathbf{k}$ with its expectation value, taken over the hole envelope function, $\phi(\mathbf{r})$.[28] That is,

$$\mathbf{k} \to -i \int \phi(\mathbf{r})\, \nabla\, \phi(\mathbf{r}) d\mathbf{r} \equiv \langle \mathbf{k} \rangle. \tag{21}$$

If the envelope function has a well-defined parity, then $\langle k_x \rangle = \langle k_y \rangle = \langle k_z \rangle = 0$, and so, from Eq. (20), $b=0$. Therefore, the Hamiltonian, Eq. (16) decouples and acts in two separate two-dimensional Hilbert spaces. We find that the hole eigenstates are given by the two pairs

$$|h_+\rangle = \sqrt{1-\epsilon^2}|J_z = +3/2\rangle + \epsilon|J_z = -1/2\rangle,$$

$$|h'_-\rangle = \sqrt{1-\epsilon^2}|J_z = -1/2\rangle - \epsilon|J_z = +3/2\rangle, \tag{22}$$

and

$$|h_-\rangle = \sqrt{1-\epsilon^2}|J_z = -3/2\rangle + \epsilon|J_z = +1/2\rangle,$$

$$|h'_+\rangle = \sqrt{1-\epsilon^2}|J_z = +1/2\rangle - \epsilon|J_z = -3/2\rangle, \tag{23}$$

where ϵ characterizes the degree of mixing. $|h_+\rangle$ and $|h_-\rangle$ are degenerate states that are predominantly heavy-holelike, and which are split from the second degenerate pair, $|h'_+\rangle$ and $|h'_-\rangle$, which have predominantly light-hole character. The nature of mixing here is quite different to the type considered in Ref. 9, where mixing between the $|J_z=+3/2\rangle$ and $|J_z=+1/2\rangle$ (or $|J_z=-3/2\rangle$ and $|J_z=-1/2\rangle$) states was assumed.

To estimate the hole mixing parameter let us now consider a specific and very simple model: that of a hole bound in a parabolic potential in all three dimensions.[30] This external potential is defined by $V(x,y,z)=(\omega_x^2x^2+\omega_y^2y^2+\omega_z^2z^2)/\gamma_1$,[26] where ω_j is the frequency of the trapping potential in the $j=\{\hat{\mathbf{x}},\hat{\mathbf{y}},\hat{\mathbf{z}}\}$ direction. We shall make the *axial approximation*, i.e., we shall ignore terms which are not axially symmetric about the z-axis; this is a good approximation for GaAs (Ref. 31) (corrections to this approximation are discussed in Ref. 32). Then the Luttinger-Kohn Hamiltonian [Eq. (16)] becomes, in the $\{|J_z=+3/2\rangle, |J_z=-1/2\rangle\}$ basis (or equivalently the $\{|J_z=-3/2\rangle, |J_z=+1/2\rangle\}$ basis):

$$\mathcal{H} = \frac{1}{4}\begin{pmatrix} 2\omega_T + \Delta E_h & W \\ W & 2\omega_T - \Delta E_h \end{pmatrix}, \tag{24}$$

where, in order to simplify notation, we have defined $\omega_T \equiv \omega_x+\omega_y+\omega_z$, $\Delta E_h \equiv (\omega_T - 3\omega_z)(\gamma_2/\gamma_1)$, and $W \equiv [\sqrt{3}(\gamma_2+\gamma_3)/2](\omega_x-\omega_y)$.

Assuming that the difference between the diagonal elements is much greater than the magnitude of the off-diagonal elements, i.e., $2\Delta E_h \gg W$, then $\epsilon \ll 1$ and is given by

$$\epsilon \approx \frac{W}{2\Delta E_h} = \frac{\sqrt{3}\gamma_1(\gamma_2+\gamma_3)(\omega_x-\omega_y)}{4\gamma_2(\omega_T - 3\omega_z)}. \tag{25}$$

As expected, the mixing is proportional to subband coupling and inversely proportional to the energy difference between the heavy and light hole subbands. Taking typical values for the Luttinger parameters for GaAs ($\gamma_1=6.8$, $\gamma_2=2.1$, and $\gamma_3=2.9$), and estimating the different trapping frequencies for an anisotropic QD to be $\hbar\omega_x=10$ meV, $\hbar\omega_y=11$ meV, and $\hbar\omega_z=45$ meV, leads to $\epsilon \approx 0.1$. We shall use this value throughout the rest of the paper.

B. Relevant trion states

We shall now assume that the hole states $|h'_+\rangle$ and $|h'_-\rangle$ are energetically distant enough from $|h_+\rangle$ and $|h_-\rangle$ that they may be ignored in our calculations of quantum dynamics (in the parabolic well model considered in the previous section this splitting is of the order of 11 meV). We are interested in using single excess spins in QDs to embody our qubit, and in exploiting spin-dependent exciton creation to couple together spins in adjacent dots. A single spin becomes a trion state[33] following the creation of an exciton, and by using Eqs. (22) and (23) we find that the trion eigenstates are

$$|x_+\rangle = |S_{\uparrow\downarrow}\rangle \otimes |h_+\rangle, \tag{26}$$

$$|x_-\rangle = |S_{\uparrow\downarrow}\rangle \otimes |h_-\rangle, \tag{27}$$

where $S_{\uparrow\downarrow}$ denotes two electrons in opposite spin states.

We emphasize that the states $|h_+\rangle$ and $|h_-\rangle$ are not eigenstates of the J_z operator, and this has profound consequences for both the coupling of charge carriers to the laser field as well as the Förster transfer interaction. We now specifically calculate the form of these two interactions.

C. Interaction with a laser field

The QD-light interaction for a (classical) laser pulse of amplitude $E(t)$ and central frequency $\omega_L(t)$ impinging on a single QD may be expressed in the dipole approximation[29] through the following Hamiltonian operator:

$$\hat{\mathcal{H}}_L(t) = eE(t)\hat{\mathbf{r}} \cdot \hat{\mathbf{n}} \cos[\omega_L(t)t], \tag{28}$$

where $\hat{\mathbf{r}}$ is the dipole operator, $\hat{\mathbf{n}}$ is the polarization vector of the light field, and e is the electronic charge. The time dependence of E and ω allows us later to introduce chirped laser pulse shapes: we assume that the time dependence is slow compared with the oscillation period of the laser.

We assume that the laser pulse has a spectral width which is narrower the typical QD level spacing. If we choose the laser frequency to be close to resonance with the ground state exciton, we can then consider an idealized model in which the dynamics is restricted only to the two qubit states defined as

$$|0\rangle = |-1/2_e\rangle,$$

$$|1\rangle = |1/2_e\rangle, \tag{29}$$

and to the trionic states $|x_+\rangle$ and $|x_-\rangle$.

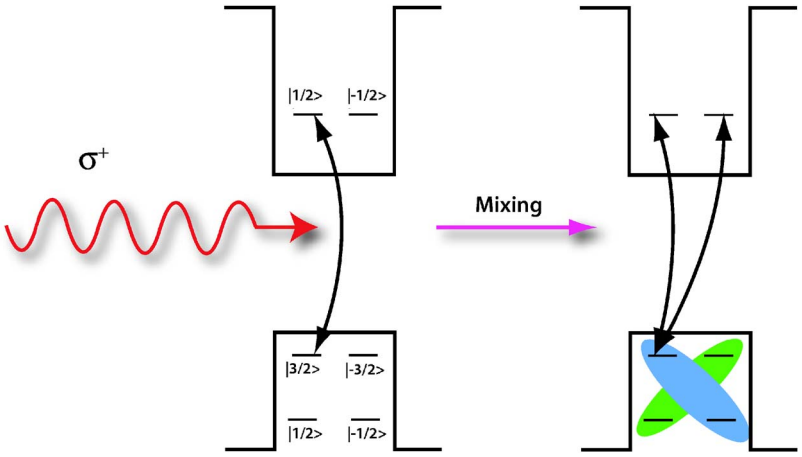

FIG. 1. (Color online) Hole states in the presence of hole subband mixing and its effect on Pauli blocking. The arrows denote the allowed optical interband transitions for an incoming σ^+ polarized laser pulse. The left part of the figure represents the situation where no hole mixing is present and the right-hand side shows the effects of mixing.

By choosing the laser pulse to be directed along z and σ^+ circularly polarized, we find that $\hat{\mathbf{r}}\cdot\hat{\mathbf{n}}=(x+iy)$. Equations (1)–(4), (10), (11), and (28) then allow us to calculate the form of the interaction between the qubit electron spin and trion states. Let us first define the length

$$l_i \equiv \int f_i(r) r^3 g(r) dr, \tag{30}$$

with $i \in \{lh, hh\}$. We also use the modified mixing parameter $\tilde{\epsilon} \equiv \epsilon(l_{lh}/l_{hh}\sqrt{3})$ and the Rabi frequency

$$\Omega(t) \equiv \frac{2eE(t)l_{hh}}{\sqrt{6}}. \tag{31}$$

Then we find, for a quantum dot labelled by κ,

$$\mathcal{H}_{\sigma^+,\kappa}(t) = \Omega(t)\cos[\omega_L(t)t](|1\rangle_\kappa\langle x_+| + \tilde{\epsilon}|0\rangle_\kappa\langle x_-| + \text{h.c.}). \tag{32}$$

In the absence of mixing ($\tilde{\epsilon}=0$) only the spin up qubit state $|1\rangle$ is coupled to the laser field; the spin down state $|0\rangle$ is completely decoupled. However, for a finite amount of hole mixing the spin-selectivity of trion excitations (required for the scheme of Ref. 10) is no longer maintained (see Fig. 1) and we must therefore consider an alternative gating strategy.

III. COUPLED QUANTUM DOT STRUCTURE

There are two principal interactions between trion states in adjacent quantum dots. The first of these is the direct Coulomb binding energy V_{XX} between two trions, which leads to the biexcitonic shift.[34] The other interaction is the off-diagonal Förster coupling, which induces the transfer of electron hole pairs, through virtual photons, and we discuss this in the following sections.

A. Angular momentum dependence of the Förster interaction

The general form of the Förster coupling Hamiltonian in QDs was discussed in detail in Ref. 35, where it was found that the magnitude of the interaction is given by

$$V_F = \frac{e^2}{4\pi\epsilon_0\epsilon_r R^3} W_1 W_2 \left(\langle \mathbf{r}_1\rangle \cdot \langle \mathbf{r}_2\rangle - \frac{3}{R^2}(\langle \mathbf{r}_1\rangle \cdot \mathbf{R})(\langle \mathbf{r}_2\rangle \cdot \mathbf{R}) \right), \tag{33}$$

where $\mathbf{R}$ is the vector connecting the centers of the two QDs. The term $\langle \mathbf{r}_i\rangle$ represents the interband expectation value of the atomic position operator for dot i,

$$\langle \mathbf{r}_i\rangle = \int_{\text{cell,dot } i} U_e(\mathbf{r}) \mathbf{r} U_h(\mathbf{r}) d\mathbf{r}, \tag{34}$$

where the U_e and U_h represent the Bloch functions for electrons and holes within dot i. The W_i represent the overlap of the envelope functions ϕ_e and ϕ_h for dot i,

$$W_i = \int_{\text{space}} \phi_e^i(\mathbf{r}) \phi_h^i(\mathbf{r}) d\mathbf{r}. \tag{35}$$

An experiment would typically be performed on a pair of *vertically stacked* quantum dots, where the vector $\mathbf{R}$ lies along the growth direction z: by using this in Eq. (33), it is easy to show that the Förster interaction conserves the angular momentum of transferring excitons. However, the nature of the exciton state before and after the transfer affects the magnitude V_F: By substituting the Bloch functions of Eqs. (1)–(6) into Eq. (33) and using the relations of Eqs. (12)–(15), we can obtain the strength of the Förster coupling for excitons which are composed of electrons and holes of varying angular momentum. We defined

$$M_{ij} = \frac{e^2}{12\pi\epsilon_0\epsilon_r R^3} W_1 W_2 l_i l_j, \tag{36}$$

for $i,j \in \{lh, hh\}$. Table I then shows the matrix element for all transitions which are induced by the Förster interaction.

B. Förster interaction for coupled trions

We next derive the form of the Förster transfer operator $\hat{T}$ for two coupled trions. The most general definition of $\hat{T}$ is

TABLE I. Relative size of the matrix element for exciton states coupled by the Förster interaction. M is defined in Eq. (36).

State 1 $(J_{z,h},J_{z,e})$	State 2 $(J_{z,h},J_{z,e})$	Matrix element	Net J_z
$-\frac{3}{2};\frac{1}{2}$	$-\frac{3}{2};\frac{3}{2}$	$M_{hh,hh}$	$-1\leftrightarrow-1$
$\frac{3}{2};-\frac{1}{2}$	$\frac{3}{2};-\frac{1}{2}$	$M_{hh,hh}$	$+1\leftrightarrow+1$
$-\frac{1}{2};\frac{1}{2}$	$-\frac{1}{2};\frac{1}{2}$	$-4M_{lh,lh}/3$	$0\leftrightarrow0$
$\frac{1}{2};-\frac{1}{2}$	$\frac{1}{2};-\frac{1}{2}$	$-4M_{lh,lh}/3$	$0\leftrightarrow0$
$-\frac{1}{2};\frac{1}{2}$	$\frac{1}{2};-\frac{1}{2}$	$4M_{lh,lh}/3$	$0\leftrightarrow0$
$-\frac{1}{2};-\frac{1}{2}$	$-\frac{1}{2};-\frac{1}{2}$	$M_{lh,lh}/3$	$-1\leftrightarrow-1$
$\frac{1}{2};\frac{1}{2}$	$\frac{1}{2};\frac{1}{2}$	$M_{lh,lh}/3$	$+1\leftrightarrow+1$
$-\frac{3}{2};\frac{1}{2}$	$-\frac{1}{2};-\frac{1}{2}$	$M_{lh,hh}/\sqrt{3}$	$-1\leftrightarrow-1$
$\frac{3}{2};-\frac{1}{2}$	$\frac{1}{2};\frac{1}{2}$	$M_{lh,hh}/\sqrt{3}$	$+1\leftrightarrow+1$

$$\hat{T}=\sum_{i,j,k,l}V_F^{i,j,k,l}(|J_{z,e}^i,J_{z,h}^j;\mathrm{vac}\rangle\langle\mathrm{vac};J_{z,e}^k,J_{z,h}^l|+\mathrm{h.c.}),\quad(37)$$

where $V_F^{i,j,k,l}$ is the size of the Förster matrix element which connects an electron and hole on dot 2 (whose angular momentum states are labelled with indices k and l) to an electron and hole and dot 1 (whose angular momentum states are labelled with indices i and j). The only nonzero values of $V_{i,j,k,l}^F$ are given in Table I, and we use that table to work out the effect of $\hat{T}$ on states in our two-dot system. For example, we have that

$$\begin{aligned}\hat{T}|1x_+\rangle&=\hat{T}\left|+\frac{1}{2}_e;+\frac{3}{2}_h,S_{\uparrow\downarrow}\right\rangle+\epsilon\left|+\frac{1}{2}_e;-\frac{1}{2}_h,S_{\uparrow\downarrow}\right\rangle\\&=M_{hh,hh}\left|+\frac{3}{2}_h,S_{\uparrow\downarrow};+\frac{1}{2}_e\right\rangle\\&\quad+\frac{\epsilon M_{lh,lh}}{3}\left|-\frac{1}{2}_h,S_{\uparrow\downarrow};+\frac{1}{2}_e\right\rangle\\&\quad+\frac{4\epsilon M_{lh,lh}}{3}\left|+\frac{1}{2}_h,S_{\uparrow\downarrow};-\frac{1}{2}_e\right\rangle.\end{aligned}\quad(38)$$

We can now see that

$$\langle x_+1|\hat{T}|1x_+\rangle=M_{hh,hh}+\frac{\epsilon^2M_{lh,lh}}{3},\quad(39)$$

$$\langle x_-0|\hat{T}|1x_+\rangle=\frac{4\epsilon^2M_{lh,lh}}{3}.\quad(40)$$

Similar calculations allow us to find all of the Förster coupling terms, which may be expressed by the following Hamiltonian, correct to first order in ϵ,

$$\begin{aligned}\mathcal{H}_F&=M_{hh,hh}(|0x_-\rangle\langle x_-0|+|1x_+\rangle\langle x_+1|)\\&\quad+\frac{2M_{hh,lh}\epsilon}{\sqrt{3}}(|1x_-\rangle\langle x_+0|+|x_-1\rangle\langle 0x_+|)+\mathrm{h.c.}\end{aligned}\quad(41)$$

C. Full Hamiltonian

The total Hamiltonian of the two QD system in the presence of laser excitation may now be written as

$$\begin{aligned}\mathcal{H}_T(t)&=\sum_{\kappa=a,b}[\delta|1\rangle_\kappa\langle 1|+\omega_{X_\kappa}\hat{P}_{X_\kappa}+\mathcal{H}_{\sigma^+,\kappa}(t)]+\mathcal{H}_F\\&\quad+\sum_{\nu,\mu\in\{x_+,x_-\}}V_{XX}(|\nu\mu\rangle\langle\nu\mu|).\end{aligned}\quad(42)$$

The state $|00\rangle$ sets the zero of energy, and then the first term describes the Zeeman energy splitting δ of the spin qubits; the second term represents the trion creation energy ω_{X_κ} where $\hat{P}_{X_\kappa}\equiv|x_+\rangle_\kappa\langle x_+|+|x_-\rangle_\kappa\langle x_-|$ is the projection operator onto the single trion state located in the QD labeled by κ; the next two terms are defined by Eqs. (32) and (41), respectively, and the last term describes the static dipole-dipole binding energy between trions V_{XX}.[9,35]

We now move to a frame which is rotating at the laser frequency ω_L for both spin-trion transitions, and make the rotating wave approximation (RWA). We then find that

$$\begin{aligned}\mathcal{H}_T(t)&=\sum_{\kappa=a,b}[\delta|1\rangle_\kappa\langle 1|+\Delta_\kappa(t)\hat{P}_{X_\kappa}+\mathcal{H}'_{\sigma^+,\kappa}(t)]+\mathcal{H}_F\\&\quad+\sum_{\nu,\mu\in\{x_+,x_-\}}V_{XX}|\nu\mu\rangle\langle\nu\mu|,\end{aligned}\quad(43)$$

where ω_{X_κ} has now been replaced by the time dependent detuning of the laser from the spin to trion transition energy $\Delta_\kappa(t)\equiv\omega_{X_\kappa}-\omega_L(t)$. The charge-laser field coupling is now given by

$$\mathcal{H}'_{\sigma^+,\kappa}(t)=\frac{\Omega(t)}{2}(|1\rangle_\kappa\langle x_+|+\tilde{\epsilon}|0\rangle_\kappa\langle x_-|+\mathrm{h.c.}).\quad(44)$$

The Hamiltonian, Eq. (43), spans a 16-dimensional Hilbert space. It is composed of the four computational basis states ($|00\rangle$, $|01\rangle$, $|10\rangle$, and $|11\rangle$), eight single trion states, and four double trion states. In order to get a little more insight into the behavior of the system, we plot its eigenenergies as a function of the ratio Δ/Ω in Fig. 2. There are three main groups of curves that are well separated away from $\Delta/\Omega=0$ (i.e., when $|\Delta/\Omega|\gg1$); these groups are simply the four computational basis states, eight single trion states and four double trion states. As Δ/Ω approaches zero (i.e., when the laser becomes resonant with the spin to trion transition energies), the eigenstates become superpositions involving different numbers of trions, and many anticrossings can be seen in the eigenstate spectrum.

IV. ADIABATIC QUANTUM GATES

In this section, we shall describe how an adiabatic change in the ratio Δ/Ω can allow us to follow the eigenstate curves. Not all of the computational basis states mix in the same way with trions when Δ/Ω is small. Following Ref. 9, it is possible to use chirped laser pulses to slowly vary Δ/Ω, which causes a nontrivial two qubit operation via trion state anticrossings.

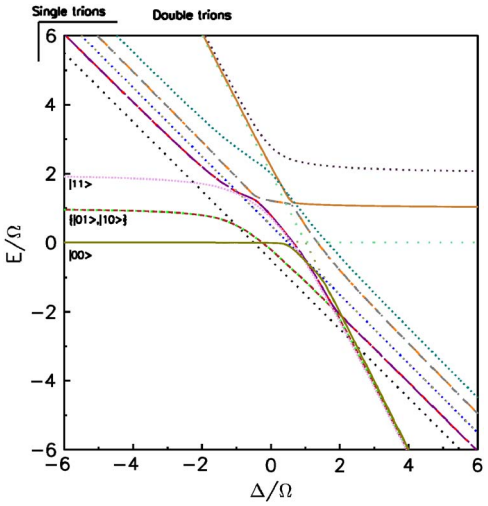

FIG. 2. (Color online) Eigenstate energy spectrum. The parameters are set as follows: $\delta/\Omega=1$, $M_{hh,hh}/\Omega=M_{lh,hh}/\Omega=0.5$, $V_{XX}/\Omega=2$, $\epsilon=0.1$.

A. Chirped pulses

Let us consider such a chirped laser pulse, where the detuning varies in time as follows:

$$\Delta(t) = -\Delta_0\left(1 - \tfrac{1}{2}e^{-(t/\tau_\Delta)^2}\right). \tag{45}$$

Δ_0 represents the maximum detuning and τ_Δ is a parameter characterizing the time variation of the detuning.

The time dependence of the laser intensity is assumed to cause the Rabi frequency to take the following form:

$$\Omega(t) = \Omega_0 e^{-(t/\tau_\Omega)^2}, \tag{46}$$

where, similarly, Ω_0 represents the maximum Rabi frequency and τ_Ω is a parameter characterizing its time variation. For a review of experimental methods for pulse shaping, see Ref. 36.

We calculate the quantum dynamics caused by our Hamiltonian with these time-varying laser pulses by using a numerical Schrödinger equation solver. If the adiabatic approximation holds true, population will return to the initial state at the end of the operation (nonadiabatic corrections limit the gate fidelity and are described below). However, the phase accumulated during the gate varies depending on the initial state. We characterize the gate by looking at the relative phase θ gained when the pulse is applied to each of the four computational basis states in turn[9]

$$\theta \equiv \phi_{00} - \phi_{01} - \phi_{10} + \phi_{11}, \tag{47}$$

where ϕ_n is the phase change of $|n\rangle$ during the gate operation. The relative phase θ is the part of the phase which is invariant under single qubit operations (see Ref. 37 for a detailed discussion). We can see this by considering the effect of the following gates. First,

$$U_1 = \begin{pmatrix} e^{-i\phi_{00}} & 0 \\ 0 & e^{-i\phi_{10}} \end{pmatrix} \tag{48}$$

is performed on qubit 1 (in the $|0\rangle$, $|1\rangle$ basis), and then

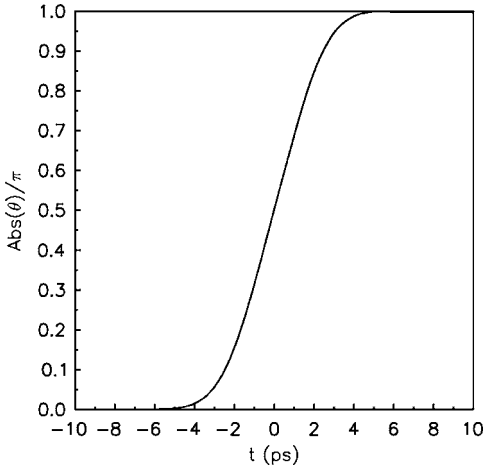

FIG. 3. Variation of θ [Eq. (47)] as a function of time. The parameters are set as follows: $\delta=1$ meV, $M_{hh,hh}=M_{lh,hh}=0.5$ meV, $V_{XX}=2$ meV, $\epsilon=0.1$, $\tau_\Omega=3.55$ ps, $\tau_\Delta=2.55$ ps, $\Delta_0=4.5$ meV, and $\Omega_0=8$ meV.

$$U_2 = \begin{pmatrix} 1 & 0 \\ 0 & e^{i(\phi_{00}-\phi_{10})} \end{pmatrix} \tag{49}$$

is performed on qubit 2. These two single qubit gate operations remove any phase picked up on the states $|00\rangle$, $|01\rangle$, and $|10\rangle$, with $|11\rangle$ undergoing a net phase change of θ. In the basis $|00\rangle$, $|01\rangle$, $|10\rangle$, $|11\rangle$, a CPHASE gate is

$$U_{\text{CPHASE}} = \begin{pmatrix} 1 & 0 & 0 & 0 \\ 0 & 1 & 0 & 0 \\ 0 & 0 & 1 & 0 \\ 0 & 0 & 0 & -1 \end{pmatrix}. \tag{50}$$

This can be constructed from any gate operation in which $\theta=\pi$, together with appropriate single qubit gates.[10]

A strength of our approach is that a phase gate can be performed whether the interdot coupling takes the diagonal form (biexcitonic interaction) or an off-diagonal form (Förster transfer). We can illustrate this by performing numerical simulations in two limits. First, we consider the case where $V_{XX} > M_{hh,hh}=M_{lh,hh}$. In this case the required phase is given predominantly through the biexcitonic coupling. If we take the same parameters as used for Fig. 2, with chirped pulses characterized by $\tau_\Omega=3.55$ ps, $\tau_\Delta=2.55$ ps, $\Delta_0=4.5$ meV, and $\Omega_0=8$ meV, then we can indeed obtain $\theta=\pi$. This is shown in Fig. 3, which displays the time dependence of θ. The population of each computational basis state (following initialization into that state) is displayed in Fig. 4; the chirped pulse moves some of the population out of each state (and into trion states) and then back again. The effect of the pulse is the same for $|01\rangle$ and $|10\rangle$, as would be expected on further inspection of our Hamiltonian. However, there is a distinct difference between the behavior of these two states and that of the states $|00\rangle$ and $|11\rangle$—and it is this difference which allows the relative entangling phase θ to be picked up.

We now move to the second case, where $V_{XX}=0$. We use the parameters $\delta=1$ meV, $M_{hh,hh}=M_{lh,hh}=0.5$ meV, $V_{XX}=0$, $\Omega_0=8$ meV, $\tau_\Omega=4.2$ ps, $\tau_\Delta=3$ ps, $\Delta_0=3$ meV, and $\epsilon=0.1$; in

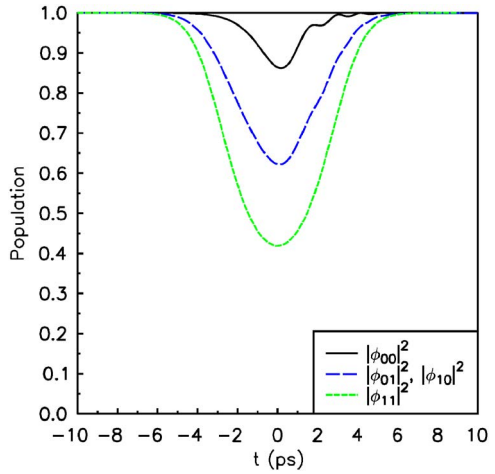

FIG. 4. (Color online) Variation of the initial state population for each computational basis state during a gate operation. The parameters are the same as in Fig. 3.

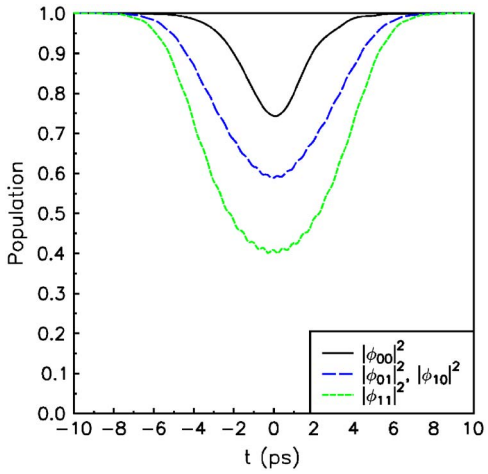

FIG. 6. (Color online) Variation of the initial state population for each computational basis state during a gate operation. The parameters are the same as in Fig. 5.

Figs. 5 and 6 we show the time variation of θ and the variation of basis state populations. We can see that it is possible to pick up an entangling phase ($\theta=\pi$) in this case too, and the effect now relies solely on the Förster interaction.

B. Gate fidelity

The gate fidelity is limited by a number of factors including: corrections to our effective four level QD model, spontaneous emission from excited states, coupling of the charge carriers to the underlying lattice which is responsible for coupling to phonons, and the possibility of nonadiabatic transitions due to the finite gate operation time.

Corrections to the effective four level QD model can be approximated as exponentially small in the ratio of the spectral width of laser pulse to the energy level spacing. As we discussed in Sec. II C, this ratio is much smaller than unity, and the reduction in the fidelity due to excitation to higher energy levels of the QDs can be safely ignored.

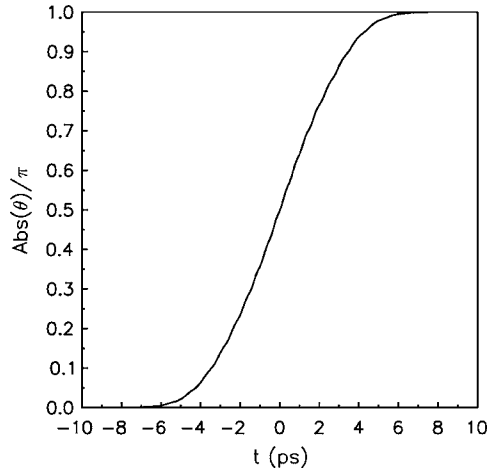

FIG. 5. Variation of θ [Eq. (47)] as a function of time. The parameters are set as follows: δ=1 meV, $M_{hh,hh}=M_{lh,hh}$=0.5 meV, V_{XX}=0, Ω_0=8 meV, τ_Ω=4.2 ps, τ_Δ=3 ps, Δ_0=3 meV, and ϵ=0.1.

It was shown in Ref. 9 that, as well as avoiding difficulties due to hole mixing, the adiabatic gating scheme also avoids further unwanted transitions related to phonon decoherence. However, since the gate is operated in a finite time, which one wishes to minimize, there are necessarily nonadiabatic transitions between the laser dressed states. Such nonadiabatic transitions are described by the Landau-Zener (LZ) theory.[38] If we assume a constant rate of change for the detuning, i.e., $\Delta(t)=\dot{\Delta}t$, the condition for adiabaticity is given by $\Omega^2/\dot{\Delta}\gg 1$, where Ω is the energy separation of the levels at closest approach. The probability for an unwanted transition by $P=\exp(-\pi\Omega^2/4\dot{\Delta})$. There is a simple physical interpretation of this:[9] $\tau\sim\Omega/\dot{\Delta}$ is the characteristic time of sweep through the resonance, and so the adiabatic condition is naturally $\Omega\tau\gg 1$. In the nonlinearized version of LZ theory the dependence of the unwanted transition is still an exponentially small function of both the reciprocal of the energy difference between the two levels ($\Delta E_{\alpha\beta}\sim 1/\Omega_{\alpha\beta}$ where α, β are two general QD states) and the characteristic sweep time τ. The proposed adiabatic gate scheme is based on the fact that the different avoided crossings between the laser dressed states can be easily distinguished, i.e., different avoided crossings occur for different values of detunings Δ and energies E (see Fig. 2). For the adiabatic gate scheme in the limit $M_{hh,hh}=M_{lh,hh}<V_{XX}$ the relevant Rabi frequency is the coupling between the states, $|00\rangle$, and $|11\rangle$ when $\Delta\approx 0$, which is the biexcitonic shift V_{XX}. Therefore one can estimate the probability of unwanted transitions to be around 10^{-6} for a typical sweep time of $\tau\sim 4$ ps. For the case in which the gate is based solely on the Förster transfer interaction $M_{hh,hh}=M_{lh,hh}=0.5$ meV the fidelity is lower and the probability of unwanted transitions for the same typical sweep time is of the order of a few percent. In order to get a better gate fidelity for the gate based on Förster interaction the typical sweep time τ should be made longer.

The adiabatic gate procedure may also reduce the effects of phonon decoherence.[9] If the gate is operated in the biexcitonic mode the probability of unwanted transitions and de-

crease in pure dephasing decoherence effects[39–41] is expected to be of the form

$$P \sim \frac{J(\omega_m)}{\Omega} \exp(-\lambda \Omega \tau), \tag{51}$$

where λ is a positive constant of order unity and $J(\omega_m)$ is the spectral function that describes the coupling of phonons to our system evaluated at some high-frequency cut-off ω_m that is imposed by the speed of the frequency detuning sweep.

The typical time scale for spin dephasing is of the order of μs and can be made even longer by optical pumping of nuclear spins.[42] Polarizing the nuclear spins will increase spin coherence since the main mechanism for spin dephasing is the coupling of the electronic spin to the nuclear spins.[43] Thus the ps time scale for the adiabatic gate does not constitute too strong a restriction.

V. STATE PREPARATION, MEASUREMENT, AND SCALABILITY

Though our paper focuses on an adiabatic two qubit gate scheme which allows one to resolve the difficulties arising due to hole mixing, we would like to briefly comment on the possibility for optically fulfilling the other requirements for a quantum information implementation scheme, i.e., initial state preparation, measurement, and scalability.

The essential test for any implementation scheme is of course provided by experiment. Recently there has been tremendous experimental effort and success in validating the essential stages needed for solid state quantum computation implementation schemes employing optically driven charged QDs. In a new experiment Gurudev Dutt *et al.* have demonstrated that a coherent optical field can produce coherent electronic spin states in QDs, demonstrating that these electronic spin states have life times much longer than the exciton coherence times.[44] Other experiments have shown how the spin state of the resident electron in a self-assembled InAs-GaAs QD can be written and read using circularly polarized optical pumping.[42,45] Methods for an optical read-out mechanism of the spin of an electron confined to a QD have also been theoretically suggested,[46–48] and some experimental work towards this goal has already been performed for colloidal semiconductor QDs.[49] Scalability is a potential problem, since spatial selectively of individual qubits is not possible in our system. This is because the optical wavelength of the exciting laser pulse is much larger than the interdot distance needed to couple our qubits. To optically resolve different QDs we would need to resort to energy-selective addressing methods within different QD clusters whose size can be controlled.[50] Inside each QD cluster one could spectrally differentiate a QD by applying a gate potential and inducing a Stark shift of the exciton levels.[30] Alternatively, globally applied pulses could be used within a cellular-automaton scheme.[34,51] One other possibility is that small scale processors based on our scheme could be joined together by using the exciton coupling to single photons. Linear optics techniques could then be used to entangle the states of two small processors.[51–53]

VI. SUMMARY

To summarize, we have derived the Hamiltonian for a pair of spin qubits in adjacent QDs, which are coupled by trion states. Our analysis shows that it is possible to perform a nontrivial two qubit gate in this system by using chirped laser pulses, even in the presence of hole mixing, and for two different types of interaction. In Ref. 9 it was shown that a dipole-dipole interaction can be used to mediate an adiabatic gate of this type. Our extension of that approach to include Förster processes generalizes this to cover all significant excitonic interactions in a coupled dot system.

In contrast to our previous work,[10] the gate proposed here could be performed in many different materials, since we have shown that it is generally valid for all significant excitonic interactions and for varying degrees of hole mixing. We therefore believe that demonstration experiments could be performed in the near future.

ACKNOWLEDGMENTS

This research is part of the QIP IRC www.qipirc.org (GR/S82176/01) and is supported through the Foresight LINK Award Nanoelectronics at the Quantum Edge www.nanotech.org by EPSRC (GR/R660029/01) and Hitachi Europe Ltd. G.A.D.B. thanks EPSRC for a Professorial Research Fellowship (GR/S15808/01). S.D.B. is supported by the EU projects Nanomagiqc and Ramboq. We thank S.C. Benjamin for useful and stimulating discussions. We are indebted to R. G. Beausoleil, who provided a numerical simulation code.

*Electronic address: brendon.lovett@materials.oxford.ac.uk

[1] D. Loss and D. P. DiVincenzo, Phys. Rev. A **57**, 120 (1998).
[2] C. Piermarocchi, Pochung Chen, L. J. Sham, and D. G. Steel, Phys. Rev. Lett. **89**, 167402 (2002).
[3] B. E. Kane, Nature (London) **393**, 133 (1998).
[4] A. Imamoğlu, Fortschr. Phys. **48**, 987 (2000).
[5] X. Hu and S. Das Sarma, Phys. Rev. A **61**, 062301 (2000); **64**, 042312 (2001); M. Bayer, P. Hawrylak, K. Hinzer, S. Fafard, M. Korkusinski, Z. R. Wasilewski, O. Stern, and A. Forchel, Science **291**, 451 (2001).
[6] F. Troiani, E. Molinari, and U. Hohenester, Phys. Rev. Lett. **90**, 206802 (2003).
[7] A. Imamoğlu, D. D. Awschalom, G. Burkard, D. P. DiVincenzo, D. Loss, M. Sherwin, and A. Small, Phys. Rev. Lett. **83**, 4204 (1999).
[8] E. Pazy, T. Calarco, I. D'Amico, P. Zanardi, F. Rossi, and P. Zoller, Europhys. Lett. **62**, 175 (2003).
[9] T. Calarco, A. Datta, P. Fedichev, E. Pazy, and P. Zoller, Phys. Rev. A **68**, 012310 (2003).
[10] A. Nazir, B. W. Lovett, S. D. Barrett, T. P. Spiller, and G. A. D. Briggs, Phys. Rev. Lett. **93**, 150502 (2004).
[11] T. H. Stievater, X. Li, D. G. Steel, D. Gammon, D. S. Katzer, D.

Park, C. Piermarocchi, and L. J. Sham, Phys. Rev. Lett. **87**, 133603 (2001); H. Kamada, H. Gotoh, J. Temmyo, T. Takagahara, and H. Ando, *ibid.* **87**, 246401 (2001); A. Zrenner, E. Beham, S. Stufler, F. Findeis, M. Bichler, and G. Abstreiter, Nature (London) **418**, 612 (2002).

[12] N. H. Bonadeo, J. Erland, D. Gammon, D. Park, D. S. Katzer, and D. G. Steel, Science **282**, 1473 (1998).

[13] X. Li, Y. Wu, D. Steel, D. Gammon, T. H. Stievater, D. S. Katzer, D. Park, C. Piermarocchi, and L. J. Sham, Science **301**, 809 (2003).

[14] T. Yokoi, S. Adachi, H. Sasakura, S. Muto, H. Z. Song, T. Usuki, and S. Hirose, Phys. Rev. B **71**, 041307 (2005).

[15] R. Hanson, B. Witkamp, L. M. K. Vandersypen, L. H. Willems van Beveren, J. M. Elzerman, and L. P. Kouwenhoven, Phys. Rev. Lett. **91**, 196802 (2003).

[16] V. N. Golovach, A. Khaetskii, and D. Loss, Phys. Rev. Lett. **93**, 016601 (2004).

[17] M. Kroutvar, Y. Ducommun, D. Hess, M. Bichler, D. Schuh, G. Abstreiter, and J. J. Finlay, Nature (London) **432**, 81 (2004).

[18] T. Förster, Discuss. Faraday Soc. **27**, 7 (1959).

[19] D. L. Dexter, J. Chem. Phys. **21**, 836 (1953).

[20] R. J. Warburton, C. S. Dürr, K. Karrai, J. P. Kotthaus, G. Medeiros-Ribeiro, and P. M. Petroff, Phys. Rev. Lett. **79**, 5282 (1997); V. K. Kalevich, M. Paillard, K. V. Kavokin, X. Marie, A. R. Kovsh, T. Amand, A. E. Zhukov, Yu. G. Musikhin, V. M. Ustinov, E. Vanelle, and B. P. Zakharchenya, Phys. Rev. B **64**, 045309 (2001); Gang Chen, N. H. Bonadeo, D. G. Steel, D. Gammon, D. S. Katzer, D. Park, and L. J. Sham, Science **289**, 1906 (2000).

[21] M. Bayer, A. Kuther, A. Forchel, A. Gorbunov, V. B. Timofeev, F. Schafer, J. P. Reithmaier, T. L. Reinecke, and S. N. Walck, Phys. Rev. Lett. **82**, 1748 (1999).

[22] W. Sheng and J.-P. Leburton, Phys. Status Solidi B **237**, 394 (2003).

[23] J. M. Luttinger and W. Kohn, Phys. Rev. **97**, 869 (1955).

[24] Q. Xie, A. Madhukar, P. Chen, and N. P. Kobayashi, Phys. Rev. Lett. **75**, 2542 (1995).

[25] U. Banin, Y. Cao, D. Katz, and O. Millo, Nature (London) **400**, 542 (1999).

[26] E. G. Tsitsishvili, Appl. Phys. A: Mater. Sci. Process. **66**, 189 (1998).

[27] A. J. Williamson, L. W. Wang, and A. Zunger, Phys. Rev. B **62**, 12963 (2000).

[28] P. K. Basu, *Theory of Optical Processes in Seminconductors* (OUP, Oxford, 1997).

[29] H. Haug and S. W. Koch, *Quantum Theory of the Optical and Electronic Properties of Semiconductors* (World Scientific, London, 1990).

[30] A. Nazir, B. W. Lovett, S. D. Barrett, J. H. Reina, and G. A. D. Briggs, Phys. Rev. B **71**, 045334 (2005).

[31] F. B. Pedersen and Y.-C. Chang, Phys. Rev. B **53**, 1507 (1996).

[32] A. O. Govorov, Phys. Rev. B **71**, 155323 (2005).

[33] F. Findeis, M. Baier, A. Zrenner, M. Bichler, G. Abstreiter, U. Hohenester, and E. Molinari, Phys. Rev. B **63**, 121309 (2001); D. V. Regelman, E. Dekel, D. Gershoni, E. Ehrenfreund, A. J. Williamson, J. Shumway, A. Zunger, W. V. Schoenfeld, and P. M. Petroff, *ibid.* **64**, 165301 (2001); A. Kiraz, S. Falth, C. Becher, B. Gayral, W. V. Schoenfeld, P. M. Petroff, Lidong Zhang, E. Hu, and A. Imamoğlu, *ibid.* **65**, 161303(R) (2002).

[34] E. Biolatti, I. D'Amico, P. Zanardi, and F. Rossi, Phys. Rev. B **65**, 075306 (2002).

[35] B. W. Lovett, J. H. Reina, A. Nazir, and G. A. Briggs, Phys. Rev. B **68**, 205319 (2003).

[36] W. S. Warren, H. Rabitz, and M. Dahleh, Science **259**, 1581 (1993).

[37] D. Vager, B. Segev, and Y. B. Band, quant-ph/0505199.

[38] L. D. Landau, Phys. Z. Sowjetunion **2**, 46 (1932); G. Zener, Proc. R. Soc. London, Ser. A **137**, 696 (1932); E. C. G. Stueckelberg, Helv. Phys. Acta **5**, 369 (1932).

[39] B. Krummheuer, V. M. Axt, and T. Kuhn, Phys. Rev. B **65**, 195313 (2002).

[40] E. Pazy, Semicond. Sci. Technol. **17**, 1172 (2002).

[41] L. Jacak, A. Janutka, J. Krasnyj, P. Machnikowski, and A. Radosz, cond-mat/0212057 (preprint).

[42] A. S. Bracker, E. A. Stinaff, D. Gammon, M. E. Ware, J. G. Tischler, A. Shavaev, A. L. Efros, D. Park, D. Gershoni, V. L. Korenev, and I. A. Merkulov, Phys. Rev. Lett. **94**, 047402 (2005).

[43] A. C. Johnson, J. R. Petta, J. M. Taylor, A. Yacoby, M. D. Lukin, C. M. Marcus, M. P. Hanson, and A. C. Gossard, Nature (London) **435**, 925 (2005).

[44] M. V. Gurudev Dutt, J. Chang, B. Li, X. Xu, X. Li, P. R. Berman, D. G. Steel, A. S. Bracker, D. Gammon, S. E. Economou, R. Liu, and L. J. Sham, Phys. Rev. Lett. **94**, 227403 (2005).

[45] S. Cortez, O. Krebbs, S. Laurent, M. Senes, X. Marie, , P. Voisin, R. Ferriera, G. Bastard, J.-M. Gérard, and T. Amand, Phys. Rev. Lett. **89**, 207401 (2002).

[46] A. Shabaev, Al. L. Efros, D. Gammon, and I. A. Merkulov, Phys. Rev. B **68**, 201305(R) (2003).

[47] E. Pazy, T. Calarco, and P. Zoller, IEEE Trans. Nanotechnol. **3**, 10 (2004).

[48] O. Gywat, H.-A. Engel, D. Loss, R. J. Epstein, F. M. Mendoza, and D. D. Awschalom, Phys. Rev. B **69**, 205303 (2004).

[49] E. Lifshitz, L. Fradkin, A. Glozman, and L. Langof, Annu. Rev. Phys. Chem. **55**, 509 (2004).

[50] D. H. Rich, C. Zhang, I. Mukhametzhanov, and A. Madhukar, Appl. Phys. Lett. **76**, 3597 (2000).

[51] S. C. Benjamin, Phys. Rev. A **61**, 020301(R) (2000).

[52] S. D. Barrett and P. Kok, Phys. Rev. A **71**, 060310 (2005).

[53] Y. L. Lim, A. Beige, and L. C. Kwek, Phys. Rev. Lett. **95**, 030505 (2005).